High field magnetotransport and point contact Andreev reflection measurements on CuCr2Se4 and CuCr2Se3Br—Degenerate magnetic semiconductor single crystals

K. Borisov, J. Alaria, J. M. D. Coey, and P. Stamenov

Citation: Journal of Applied Physics **115**, 17C717 (2014); doi: 10.1063/1.4861683
View online: http://dx.doi.org/10.1063/1.4861683
View Table of Contents: http://scitation.aip.org/content/aip/journal/jap/115/17?ver=pdfcov
Published by the AIP Publishing

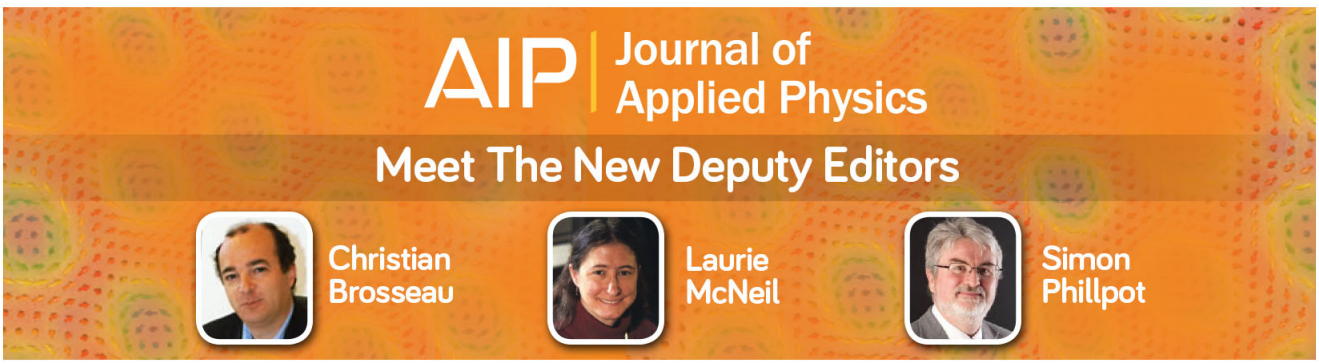

High field magnetotransport and point contact Andreev reflection measurements on $CuCr_2Se_4$ and $CuCr_2Se_3Br$—Degenerate magnetic semiconductor single crystals

K. Borisov,[1,a)] J. Alaria,[2] J. M. D. Coey,[1] and P. Stamenov[1]
[1]*School of Physics and CRANN, Trinity College, Dublin 2, Ireland*
[2]*Department of Physics, University of Liverpool, Liverpool L69 7ZE, United Kingdom*

(Presented 5 November 2013; received 23 September 2013; accepted 17 October 2013; published online 30 January 2014)

Single crystals of the metallically degenerate fully magnetic semiconductors $CuCr_2Se_4$ and $CuCr_2Se_3Br$ have been prepared by the Chemical Vapour Transport method, using either Se or Br as transport agents. The high-quality, millimetre-sized, octahedrally faceted, needle- and platelet-shaped crystals are characterised by means of high field magnetotransport ($\mu_0 H \leq 14$ T) and Point Contact Andreev Reflection. The relatively high spin polarisation observed $|P| > 0.56$, together with the relatively low minority carrier effective mass of 0.25 m_e, and long scattering time 10^{-13} s, could poise these materials for integration in low- and close-to-room temperature minority injection bipolar heterojunction transistor demonstrations. © *2014 AIP Publishing LLC*. [http://dx.doi.org/10.1063/1.4861683]

In the quest for combining semiconducting and magnetic functionality into a single material, two separate paths exist—one of the dilute magnetic semiconductors (e.g., Co:ZnO and Mn:GaAs), which is not free from controversies over the existence of secondary phases and the possibility of achieving $T_c >$ RT operation in a magnetically homogeneous system; and another of the fully magnetic semiconductors, where the structures are intrinsically magnetic, but in most cases electronically degenerate, exhibiting $T_c <$ RT, and low mobilities. Here, the magnetotransport and Point Contact Andreev Reflection (PCAR) characterisation of two degenerate fully magnetic semiconductor, single crystalline systems are described: $CuCr_2Se_4$ and $CuCr_2Se_3Br$.

The samples used for this study are prepared by Chemical Vapour Transport (CVT) in sealed fused silica vessels, using either Se_2 or $CuBr_2$ as the transport agents, at temperatures in the range of 800–900 °C, with a controlled gradient, within a two-zone growth furnace. The pure $CuCr_2Se_4$ crystals grown by this method are a mixture of habits correlating with their size. The smaller crystals ($\lesssim$300 μm in size) tend to have truncated octahedral shapes, while the bigger ones (still $\lesssim$600 μm in size) typically form agglomerated platelets, exposing the {111}, slowest growth plane. The $CuCr_2Se_3Br$ crystals are typically octahedral needles (in some cases >2500 μm in length), of varying aspect ratio (from 1:2 to 1:10), with again the {111}, being the slowest and the {110} being one of the fastest growth planes. Both systems crystallise in space group $Fd\bar{3}m$, with lattice parameters of 10.4325(2) and 10.775653(9) Å for the Br-less and Br-containing compositions, respectively, verified by single crystal X-ray diffraction. The saturation magnetisation varies between 4.75 and 5.75 μ_B/f.u., depending on Br content and preparation conditions, as determined by SQUID-based magnetometry. The cubic magnetocrystalline anisotropy constant is about 50 kJ·m^{-3}, extracted from tensoresistive chip-based torque magnetometry, in fields of up to 14 T. Curie temperatures are 430(5) K and 281(2) K, respectively, and are determined by SQUID-based AC susceptibility and are confirmed by observed heat capacity anomalies.

Samples for the transport studies are diamond-cut with $z \parallel [111]$, and 4-6 contacts are permanently indium-soldered. The magnetotransport is dominated by the spontaneous scattering coefficients, as illustrated on Fig. 1. The magnetoresistance peaks to just below 2% at about 150 K and are analysed (in the temperature range 2–300 K) together with the Hall effect, within a common non-linear least-squares regression model, taking into account two bands of majority and minority holes, ionised impurity scattering (IIS), and magnetic scattering (MS). Majority hole concentrations range between 3.6 and 4.8 $\times 10^{27}$ m^{-3} between 2 and 300 K, and agree well with estimates using the Drude tail observed in infrared reflectivity, and the electronic specific heat (the Debye temperature is $T_D = 305$ K). Minority hole concentrations are below about 20×10^{22} m^{-3}, at low temperature, and become immeasurable above about 100 K. Using majority and minority effective mass of 0.65 and 0.25 m_e, respectively,[1] the scattering times obtained are about 3×10^{-15} s and 1×10^{-13} s. The characteristic field scales for the IIS and MS processes are about 10 T and 0.4 T, respectively. The anisotropy of the magnetoresistance can be as high as 30% in fields of $\mu_0 H < 100$ mT and at $T = 10$ K. Again, the analysis has to be executed within a complete transport model, simultaneously for the diagonal and Hall resistivity, as illustrated on the insets of Fig. 1. The samples used for PCAR are prepared in two different fashions. For $CuCr_2Se_4$, where larger, well faceted, are not available, a small (<80 μm wide) well-formed truncated octahedron is indium-soldered to the end of a 0.5 mm diameter Cu wire and used to indent on a polished (to better than 100 nm) polycrystalline niobium surface. For $CuCr_2Se_3Br$, in contrast, a $z \parallel [111]$ platelet of lateral size (2×4 mm^2) is indented with a shear-cut polycrystalline niobium needle. In both cases, the

a)Electronic mail: borisovk@tcd.ie.

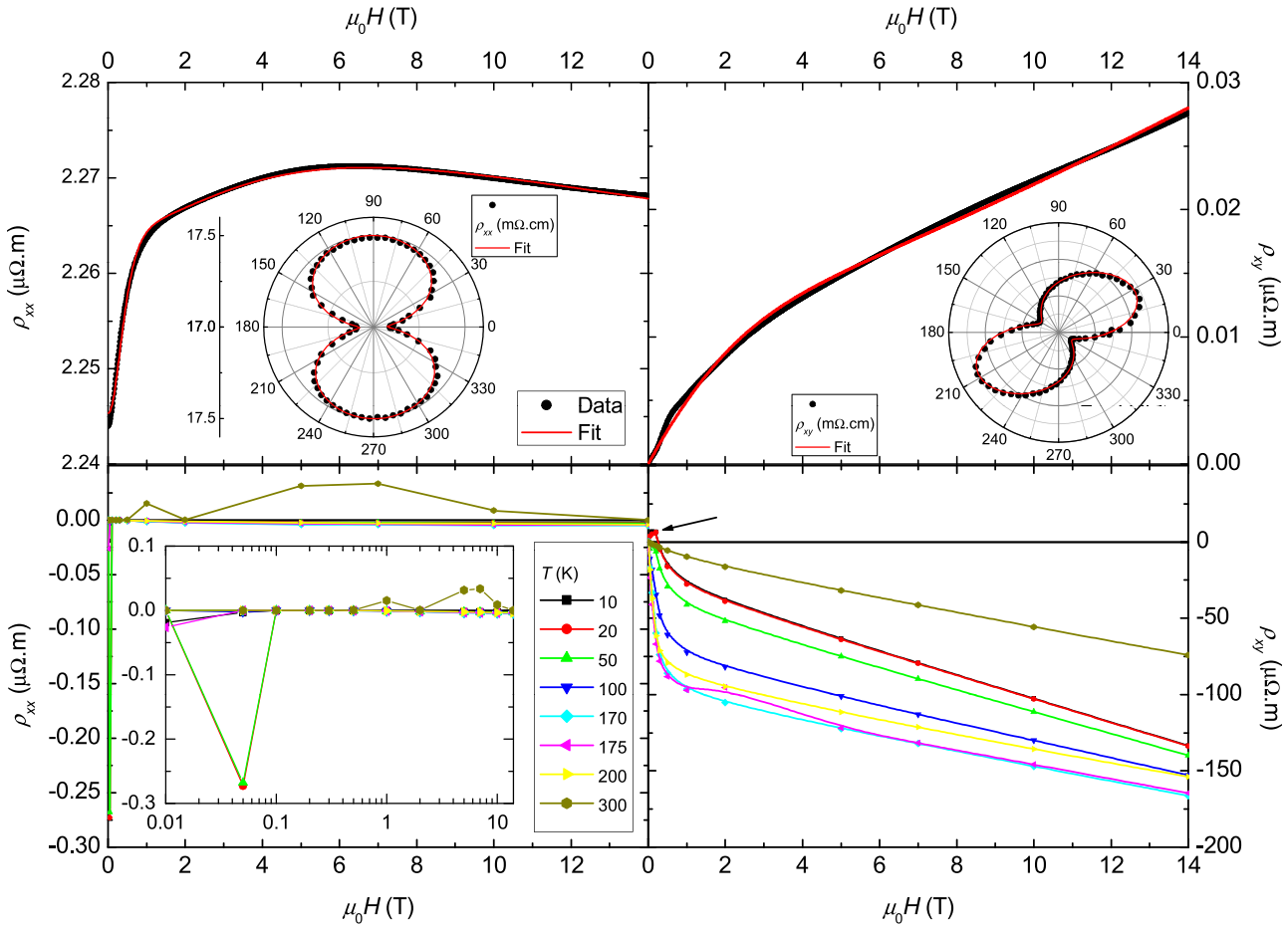

FIG. 1. Resistivity and Hall effect in $CuCr_2Se_4$ (top) and $CuCr_2Se_3Br$ (bottom). The top insets provide a view of the angular dependencies of ρ_{xx} and ρ_{xy} upon azimuthal rotation. Continuous lines on the top panel are fits. Each data point on the bottom panels is a result of a fit to a complete angular dependence. The arrow points to a physical change of phase of ρ_{xy} below ~50 K.

contacts are formed at lattice temperatures in the range from 1.8 to 15 K, in a He vapour-flow through sample space cryostat (Oxford instruments). Magnetic field is applied by a "Multimag" permanent-magnet-based variable-flux source, capable of providing up to $\mu_0 H = 1$ T, in any direction within the plane normal to the dominant current direction (z-axis). As there are inevitably uncompensated magnetic field components at the sample (<0.5 mT), definite magnetisation state is imparted on both samples on cool-down. The relative translation of the superconductor with respect to the sample, required for the formation of the point contacts, is provided by a combination of differential micrometer drive and a single-axis piezo positioner. The construction of the PCAR setup is similar to

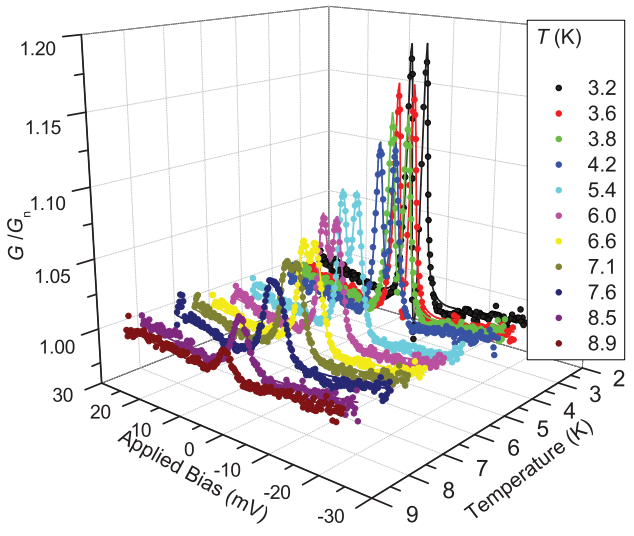

FIG. 2. Conductance spectra of a Nb/$CuCr_2Se_3Br$ contact at $\mu_0 H = 0.0$ mT and various temperatures $3 < T < 9$ K. Continuous curves are fits using a $T_e = T$ fix for the electronic temperature, with $\Delta_1 \sim 1.4$ meV.

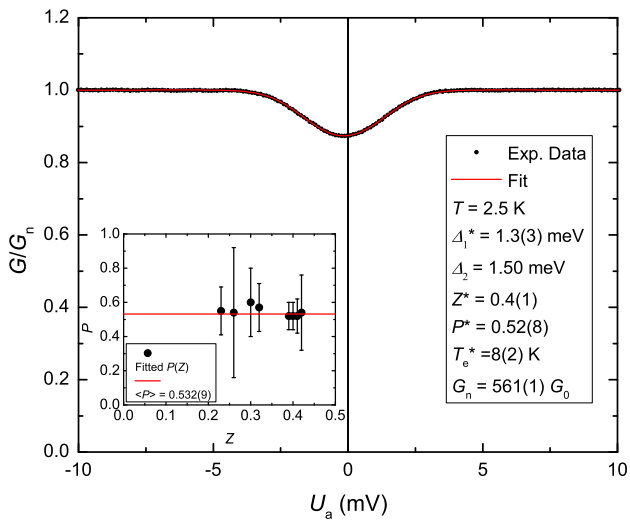

FIG. 3. Conductance spectra of a $CuCr_2Se_4$/Nb contact at $\mu_0 H = 0.0$ mT. The inset shows the variation of $P(Z)$ for the successful fits.

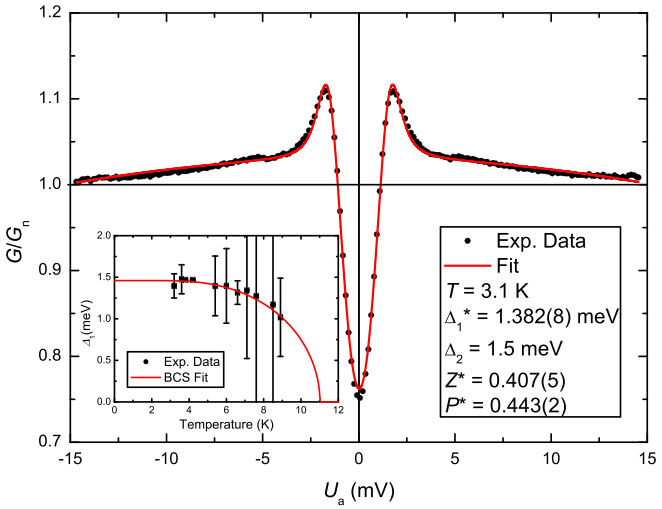

FIG. 4. Conductance spectra of a Nb/$CuCr_2Se_3Br$ contact at $\mu_0 H = 0.0$ mT. The inset shows the variation $\Delta_1(T)$, together with a (Bardeen, Cooper and Schrieffer) fit to it, with $T_c^* = 11(1)$ K and $\Delta_1^*(0) = 1.48(2)$ meV.

the ones of Ref. 2, while a description of the real-time derivative-spectrum measurement system used, and the spectral fitting software can be found in Ref. 3, for the case of $CuCr_2Se_3Br$, and in Refs. 4 and 5, for $CuCr_2Se_4$. Fig. 2 presents an example of the temperature evolution of the derivative spectra for the Br-containing composition. All spectra are successfully fitted within the framework of the well-known modified (Blonder, Tinkham and Klapwijk)[6] theory, using the methodology attributed to,[7] further taking into account superconducting proximity, electronic heating, modulation broadening, and series resistance. A number of contacts are formed to the same sample surface and the contact exhibiting the largest evaluated polarisation $|P|$ is then quoted. No specific extrapolations, such as the ones described in Ref. 8, have been performed, rather a constant value of the polarisation is assumed, as illustrated in the inset of Fig. 3, thus taking a pessimistic limit for $|P|$. The uncertainties of the derived parameters are evaluated, following a conventional approach utilizing Jacobian derivative matrices,[5] and further corrected using Student's *t*-distribution. Throughout this study a diffusive definition of $|P|$ is used,[9] where the density of states (DOS) is $\vec{v}^2_{\uparrow\downarrow}$ velocity averaged around the Fermi level E_F. There is no clear statistical justification for analysing any of the PCAR spectra, measured here, within a ballistic framework.

Spin polarisation is inferred to be $|P| = 0.532(9)$ and 0.443(1), respectively, in the temperature interval 1.9–9.0 K. Proximity gaps are $\Delta_1 = 1.2$–1.4 meV. Delta-barrier strengths observed are $Z = 0.20$–0.41, all illustrated on Figs. 3 and 4.

Contact size is controlled by varying contact pressure, in order to produce different contacts (in terms of their parameters *Z*, *P*, etc.) as illustrated on the inset of Fig. 3, however, this is often not a monotonic process, and especially in the reversed geometry (the case of $CuCr_2Se_4$), where the sample acts as the indenting tip, leads to dislocation propagation, cracking, and eventually macroscopic fracturing of the crystal. In the limiting case, the contact does no longer contain a single weak link, and the nominal interpretation requires two or more discrete point contact models.[10] Here, these have been excluded, even though some are actually interpretable within extended fitting models (see Ref. 4). The contacts formed on $CuCr_2Se_3Br$ are much more stable and reproducible being formed in the conventional Nb tip geometry.

Magnetic field of up to $\mu_0 H \leq 1$ T is found to only weakly alter the observed conductance spectra, well below $T_c = 9.2$ K, by widening the observed spectral features, for both single crystals, likely on the account of the relatively large expected domain size. No further analysis of the field dependencies is therefore performed here.

Despite their electronic degeneracy (without any additional quaternary doping of In, Ga, or Ag), $CuCr_2Se_4$ and $CuCr_2Se_3Br$ exhibit useful low-temperature mobility and high Fermi level spin polarisation, while providing a useful magnetic moment in excess of 5 μ_B/f.u. Future bipolar doping of these magnetic semiconductors in thin film form should lead to useful spin-electronic functionality close to and above room temperature.

Useful discussions with M. Venkatesan are gratefully acknowledged, as is financial support from Science Foundation Ireland, within the SSPP (11/SIRG/I2130), NISE (10/IN1/I3002), and AMBER programmes.

[1]J. S. Bettinger, R. V. Chopdekar, M. Liberati *et al.*, J. Magn. Magn. Mater. **318**, 65 (2007).
[2]R. J. Soulen, M. S. Osofsky, B. Nadgorny *et al.*, J. Appl. Phys. **85**, 4589 (1999).
[3]P. Stamenov and J. M. D. Coey, J. Appl. Phys. **109**, 07C713 (2011).
[4]P. Stamenov, J. Appl. Phys. **111**, 07C519 (2012).
[5]P. Stamenov, J. Appl. Phys. **113**, 17C718 (2013).
[6]G. E. Blonder, M. Tinkham, and T. M. Klapwijk, Phys. Rev. B **25**, 4515 (1982).
[7]R. J. Soulen, J. M. Byers, M. S. Osofsky *et al.*, Science **282**, 85 (1998).
[8]M. Stokmaier, G. Goll, D. Weissenberger, C. Sürgers, and H. v. Löhneysen, Phys. Rev. Lett. **101**, 147005 (2008).
[9]I. I. Mazin, Phys. Rev. Lett. **83**, 1427 (1999).
[10]V. Baltz, A. D. Naylor, K. M. Seemann *et al.*, J. Phys.: Condens. Matter **21**, 095701 (2009).